This article has been accepted for publication in a future issue of this journal, but has not been fully edited. Content may change prior to final publication. Citation information: DOI 10.1109/ACCESS.2017.2713459, IEEE Access

Analytical Characterisation of the Terahertz In-vivo Nano-network in the Presence of Interference based on TS-OOK Communication Scheme

Rui Zhang, *Student Member, IEEE,* Ke Yang *Member, IEEE,*, Qammer H. Abbasi, *Senior Member, IEEE,* Khalid A. Qaraqe, *Senior Member, IEEE,* and Akram Alomainy, *Senior Member, IEEE,*

***Abstract*—The envisioned dense nano-network inside the human body at terahertz frequency suffers a communication performance degradation among nano-devices. The reason for this performance limitation is not only the path loss and molecular absorption noise but also the presence of multi-user interference and the interference caused by utilising any communication scheme $e.g.$, Time Spread On-Off Keying (TS-OOK). In this paper, an interference model utilising TS-OOK as a communication scheme of the THz communication channel inside the human body has been developed and the probability distribution of Signal-to-Interference-plus-Noise Ratio (SINR) for THz communication within different human tissues like blood, skin and fat has been analysed and presented. In addition, this paper evaluates the performance degradation by investigating the mean values of SINR under different node densities in the area and the probabilities of transmitting pulses. It results in the conclusion that the interference restrains the achievable communication distance to approximate 1 mm, and more specific range depends on the particular transmission circumstance. Results presented in this paper also show that by controlling the pulse transmission probability and node density, the system performance can be ameliorated. In particular, SINR of in-vivo THz communication between the deterministic targeted transmitter and receiver with random interfering nodes in the medium improves about 10 dB, when the node density decreases one order. The SINR increases approximate 5 dB and 2 dB, when the pulse transmitting probability drops from 0.5 to 0.1 and 0.9 to 0.5, respectively.**

***Index Terms*—Interference, Body-centric Nano-networks, Signal-to-Interference-plus-Noise Ratio, Time Spread On-Off Keying**

I. Introduction

With the aim of creating nano-devices with new functionality, nanotechnology can satisfy the need to reduce the size of the devices in the network, and also motivates promising medical applications such as drug delivery and continuous health monitoring [1]. Recent developments in novel materials, like carbon nano-tube (CNT), graphene, $etc.$, encourage the electromagnetic communication among nano-devices in the THz band (0.1-10 THz) inside the human body [2], [3].

In literature, a few research activities have been conducted in characterising the channel models of nano-networks at the THz band, which are primarily focused on the single user channel models [4]–[7]. The end-to-end model is an ideal simplification of the communication channel, whereas in reality, the communication environment is much more complicated and the requirements of nano-networks widely change across applications. For example, in Wireless Nano-sensor Networks (WNSNs), very high node densities, in the order of hundreds of nano-sensors per square millimetre, are needed to overcome the limited sensing range of individual devices [8]. Moreover, different types of nano-devices could be interleaved and cooperated to conduct more complicated tasks, resulting in up to thousands of nano-machines per square millimetre.

With respect to dense nano-networks, multi-user interference will occur, when symbols from different transmitters reach the receiver at the same time and overlap. Therefore, not only the path loss and molecular absorption noise, but also the multi-user interference could be the major impairment that degrades the performance of in-vivo nano-communication at the THz band. In addition to the interference caused by different nodes in the communication area, with the utilisation of Time Spread On-Off Keying (TS-OOK), collisions between symbols can also occur. These collisions result in interference, which imposes a strict limitation on the communication channel parameters and requirements, especially the achievable distance at which nano-machines can communicate.

In order to evaluate the potential of the THz communication inside the human body, it is significantly important to conduct network-level analysis and characterise the system performance while using TS-OOK as a communication scheme. In proceed with assessing the link performance of the wireless communication, the probability distribution and mean values of Signal-to-Interference-plus-Noise Ratio (SINR) are quantified as fundamental metrics.

A preliminary investigations on the multi-user network were performed by Jornet $et\ al.$ in [9], [10], where a statistical interference model for pulse-based communication in nano-networks was proposed, taking into account the peculiarities of the THz band.

However, it is a specific case for transmitting 100 fs pulses with an energy equal to 1 pJ in air with 10% water vapour molecules, and the resulting interference model is highly dependent of the specific channel molecular composition as well as the power and the shape of the transmitted signal. When the transmission medium becomes different,

Rui Zhang, Ke Yang and Akram Alomainy are with Electronic Engineering and Computer Science, Queen Mary University of London, London (rui.zhang, k.yang, a.alomainy)@qmul.ac.uk

Qammer H. Abbasi is with School of Engineering, University of Glasgow, Glasgow qammer.abbasi@glasgow.ac.uk

Khalid A. Qaraqe is with Electrical and Computer Engineering, Texas A&M University, Qatar khalid.qaraqe@qatar.tamu.edu

This article has been accepted for publication in a future issue of this journal, but has not been fully edited. Content may change prior to final publication. Citation information: DOI 10.1109/ACCESS.2017.2713459, IEEE Access

the polynomial approximation of the received signal power used in [9] would be different, which finally changes the probability density function (pdf) of the interference power. In addition, an analytical framework for the interference and SINR estimation in dense THz networks has been proposed in [11], [12]. The interference and SINR of mm-wave and THz bands are explored by capturing the effect of the antenna directivity, radiation pattern and blocking in [13]. However, the communication scheme was not considered in [11]–[13] and the model is only valid for flat power transmission. With regards to TS-OOK communication scheme, it is believed that Gaussian pulses are transmitted for message propagation.

In this paper, an interference model and pdf for SINR of in-vivo nano-networks at the THz band using TS-OOK communication scheme are developed for network-level analysis. Without loss of generality, the developed model is valid for any power scheme. The model is based on the peculiarities of the THz signal propagating inside human tissues, while considering the modulation scheme and statistical information of interferer in the transmission medium. The pdf for SINR of the THz communication inside the human blood, skin and fat tissues for different node densities and probabilities of transmitting pulses is analytically presented. The degradation effect of the presence of interference is illustrated by investigating on the SINR mean values under different communication circumstance.

The remainder of the paper is organised as follows. In section II, a brief overview of the THz communication channel and noise models of the in-vivo nano-networks is provided. Section III presents the feasibility of TS-OOK communication scheme for in-vivo nano-communication at the THz band. In section IV, an interference model and probability distribution of SINR for in-vivo nano-networks are developed. Analytic results for pdf of SINR at different node densities and probabilities are presented in section V for different human tissues, in addition to comparative analysis of the node density and probability on system performance. Section VI highlights the conclusion.

II. End-to-End THz Propagation and Noise Models

There are a number of papers presenting channel models for the THz wave propagating in the atmosphere [4], [8], [14], [15]. The in-vivo nano-communication channel models at the THz band have been developed in [7], [16], [17]. The path loss of the THz wave inside human tissues can be divided into the spreading loss and the molecular absorption loss. The molecular absorption can be described by the absorption coefficient. The details on the calculation of the absorption coefficient and refractive index of human tissues have been discussed in [16]. The measured absorption coefficient for human blood, skin and fat tissues in literature [18], [19] are given as in Fig. 1.

The noise in the THz communication is primarily contributed by the molecular absorption noise [4]. This kind of noise is caused by vibrating molecules which partially re-radiate the energy that has been previously absorbed.The molecular absorption noise N_m for the THz communication

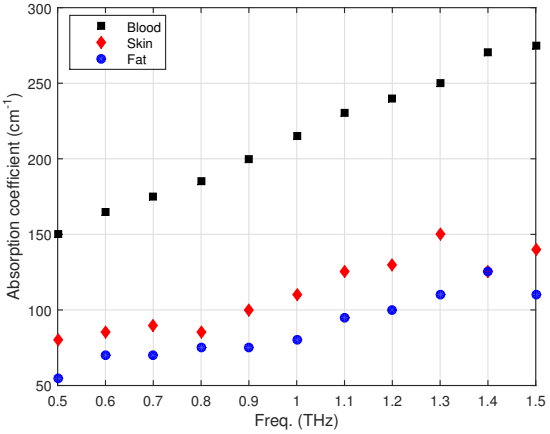

Figure 1. Measured absorption coefficient of human blood, skin and fat

in the human body is composed of the background noise N_b and the self-induced noise N_s [20], [21], and the noise power can be represented by,

$$N_b(r) = \int_B B(T_0, f)(\frac{c}{\sqrt{4\pi} n_0 f_0})^2 df \tag{1}$$

$$N_s(r) = \int_B S(f)(1 - e^{-\alpha(f)r})(\frac{c}{4\pi n f r})^2 df \tag{2}$$

$$N_m(r) = N_b(r) + N_s(r) \tag{3}$$

where B is the bandwidth of the communication channel, T_0 is the reference temperature of the medium, n is the refractive index, n_0 is the corresponding refractive index of the THz wave in the medium, when the frequency of the wave is f_0, and $\alpha(f)$ is the absorption coefficient. $B(T_0, f)$ stands for the Planck's function and $S(f)$ refers to the transmitted signal power spectral density (p.s.d) from the transmitter antenna.

The expected received signal power from the targeted transmitter in the channel can be represented by,

$$P_R(r) = \int_B S(f)(\frac{c}{4\pi n f r})^2 e^{-\alpha(f)r} df \tag{4}$$

III. Time Spread On-Off Keying for in-vivo Nano-networks in the THz band

Due to the fact that nano-devices in WNSNs are highly energy constrained with limited capabilities, it is technologically challenging for a nano-transceiver to generate a high-power carrier frequency in the THz band. Thus, the best modulation option for WNSNs is carrier-less pulse based modulation [22]. In light of the state of the art in graphene-based nano-electronics, a transmission scheme for nano-devices, based on the transmission of one-hundred-femtosecond long pulses by following an on-off keying modulation spread in time is proposed [9], named TS-OOK. These very short pulses can be generated and detected with nano-transceivers based on graphene and high-electron-mobility materials such as Gallium Nitride or Indium Phosphide [23].

TS-OOK is a communication scheme assuming that a nano-machine needs to transmit a binary stream. A logical "1" is

This article has been accepted for publication in a future issue of this journal, but has not been fully edited. Content may change prior to final publication. Citation information: DOI 10.1109/ACCESS.2017.2713459, IEEE Access

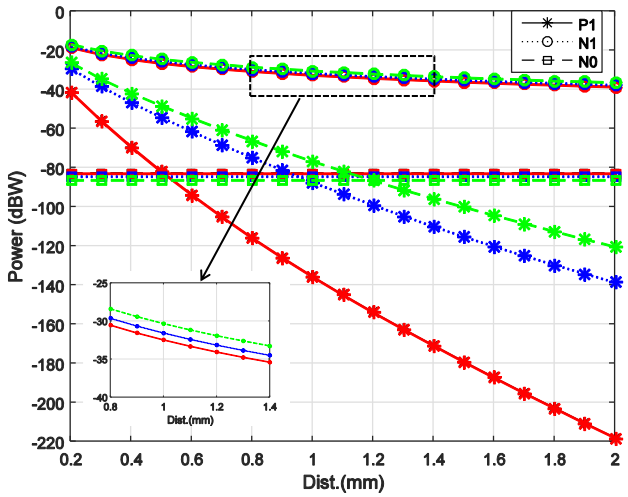

Figure 2. Power vs distance for three different human tissues. Where blood (red), skin (blue) and fat (green), P_1 (noise power when pulse is transmitted), N_1(noise power associated with a pulse) and N_0 (noise power associated with silence). The graph in the insets shows magnifications of N_1 with the distance from 0.8 mm to 1.4 mm.

transmitted by using a femtosecond-long pulse and a logical "0" is transmitted as silence. The time between symbols T_s is much longer than the symbol duration T_p. To the best authors' knowledge, TS-OOK is the most promising communication scheme for resource-constrained nano-networks.

When adopting TS-OOK as the communication scheme for nano-networks, the nano-transmitters can start transmitting at any time without being synchronised or controlled by any type of network central entity. Hence the traffic in the network can drastically increase at specific times due to correlated detection in several nano-sensors, and collisions between symbols can occur [9]. In order to proceed with the system-level investigation of in-vivo nano-networks, it is significantly important to confirm the feasibility of TS-OOK for nano-communication inside the human body.

To investigate TS-OOK communication scheme inside human tissues, a comparatively illustration of the results for both the received signal power and the noise power is presented. The received signal power is denoted as P_1 as shown in (4), when a pulse has been transmitted, while the noise power associated with the transmission of pulses and the noise power, when transmitting silence are N_1 and N_0, respectively. N_1 is the total molecular absorption noise power in (3), and N_0 is only the background noise power as shown in (1). To an extent to keep the numerical results realistic, and in light of the state of the art in molecular-electronics, the total energy and the pulse duration of the Gaussian power is equal to 1 pJ and 100 fs, respectively [4]. The derivative order and the standard deviation of the Gaussian pulse are set to 6 and 0.15, respectively. In this paper, the frequency band of interest is 0.5 THz to 1.5 THz with a bandwidth of 1 THz. The resulting power for communication inside three human tissues are represented as functions of the transmission distance as shown in Fig. 2.

It can be clearly seen from Fig. 2, compared to the received signal power, the noise power is big enough to influence the link quality. According to the results presented in [10], the received power when transmitting a pulse tends to be lower than the noise power when the transmission distance increases to 1 cm. For the case within in-vivo nano-networks at the THz band, the results are evidently different. The received signal power P_1 when a pulse is transmitted inside human tissues is always much lower than the molecular absorption noise power N_1 regardless of the type of the transmission medium. This difference could be explained by the fact that the molecular absorption coefficient inside human tissues is thousands times of that in air [4], [16], which causes a much more significant attenuation to the signal. In addition, it is noticed that the noise power associated with the transmission of silence is constant with distance, because only the background noise is present in this case and the background noise is independent of the signal transmission. More importantly, even if the power of the received signal tends to zero, the noise power caused by the propagating pulse keeps much higher than the background noise power. In other words, when a pulse is transmitted, the received power including both the targeted signal power P_1 and the molecular absorption noise power N_1 is always much higher than the power of the silence case whatever human tissues are considered. Thus, it is clear for the receiver that a pulse was transmitted provided that the molecular absorption noise power is detected, which means that the logical "1" and logical "0" can be clearly detected, which reduces the error probability for in-vivo nano-networks. The obtained results demonstrate the feasibility of TS-OOK as a communication scheme for the THz communication inside the human body. Moreover, since the received signal power is directly proportional to the transmitted signal power, reasonable transmission power needs to be chosen to keep the power at the receiver much higher with transmitting pulses than the power with transmitting silence to make the signal detection more accurate.

IV. Multi-user Scenario for In-vivo Nano-communication

In this section, an interference model which is valid to any kind of power allocation scheme is introduced. Besides, the probability distribution and mean values of SINR are derived for THz communication inside the human body with the presence of multiple interferer in dense nano-networks. The investigation captures the unique characteristics of the THz band channel inside human tissues and the properties of TS-OOK communication scheme.

A. System Model

Generally, a random nodes deployment in R^2 as shown in Fig. 3 is used for performance assessment of cellular, ad-hoc and device-to-device networks [24]. The targeted receiver is assumed to be at the center of the disc, while the targeted transmitter locates at a distance r_0 from the receiver. All the other nodes in this field are considered as interfering nodes for the targeted receiver. Following most studies, Possion Point Process (PPP) is utilised to provide first order approximation of nodes positions within a disc of radius R [25]. Thus, the

This article has been accepted for publication in a future issue of this journal, but has not been fully edited. Content may change prior to final publication. Citation information: DOI 10.1109/ACCESS.2017.2713459, IEEE Access

probability of finding M nodes in the area $A(R)$ can be represented as [26],

$$P[M|A(R)] = \frac{(\lambda\pi R^2)^M}{M!}e^{-\lambda\pi R^2} \quad (5)$$

where λ refers to the node density in $nodes/m^2$. The mean and variance of the number of interferer M can be written as [26],

$$E[M] = \lambda\pi R^2, \sigma^2[M] = \lambda\pi R^2 \quad (6)$$

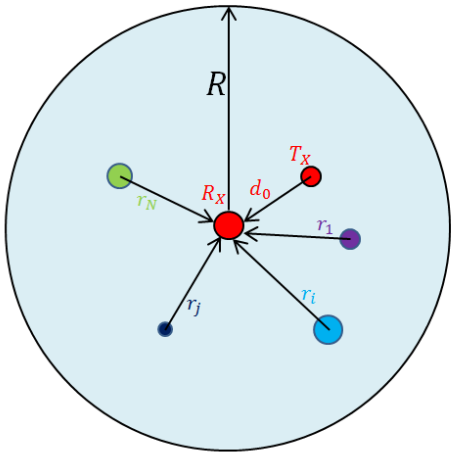

Figure 3. Nano-devices deployment inside body for multi-user scenario

B. Moments and Distribution of SINR

SINR is an important metric to evaluate the system performance of the dense nano-networks. The instantaneous frequency-dependent SINR is defined as,

$$SINR(\vec{r}, S, f, \lambda) = \frac{P_R(r_0, S, f)}{I(\vec{r}, S, f, \lambda) + N(\vec{r}, S, f, \lambda)} \quad (7)$$

where $\vec{r}$ is the vector of distances $r_i, i = 1, 2, ..., M$, standing for the separation distances between the interferer and the targeted receiver, S is the p.s.d of the transmitted signal power and M is the number of interfering nodes. f is the operating frequency and λ is the intensity of interferer. $P_R(r_0, S, f)$ refers to the targeted receiver signal power, while $I(\vec{r}, S, f, \lambda)$ denotes the aggregate power of the interfering signals at the targeted receiver and $N(\vec{r}, S, f, \lambda)$ is the noise power at the targeted receiver including all the noise power caused by the targeted transmitter and interferer. In this paper it is assumed that there is no power control capabilities, which means that $S_i = S_j = S, i, j = 0, 1, ..., M$ [11], [12]. For simplicity, in the following, we drop arguments of notation that are often silently assumed, f, S and λ. The aggregate interference from M sources is given by [12],

$$I(\vec{r}) = \sum_{i=1}^{M} \int_B S(f)(\frac{c}{4\pi nf})^2 r_i^{-2} e^{-\alpha(f)r_i} df \quad (8)$$

where $S(f)$ is the transmitted signal p.s.d from the transmitter antenna. The noise power is written as a summation of the noise caused by both the targeted transmitter and the interfering nodes in the communication area,

$$N(\vec{r}) = N_m + \sum_{i=1}^{M} \int_B S(f)(\frac{c}{4\pi nf})^2 r_i^{-2}(1 - e^{-\alpha(f)r_i}) df \quad (9)$$

where N_m is the molecular absorption noise power obtained from (3). Substituting (8) and (9) into equation (7) gives,

$$SINR(\vec{r}) = \frac{P_R}{N_m + \sum_{i=1}^{M} \int_B S(f)(\frac{c}{4\pi nf})^2 r_i^{-2} df} \quad (10)$$

Whereas in (10) P_R is a constant value that can be estimated for any given distance r_0. The second term in the denominator of (10) is the only random term, which is given as,

$$X(\vec{r}) = \sum_{i=1}^{M} A r_i^{-2}, A = \int_B S(f)(\frac{c}{4\pi nf})^2 df \quad (11)$$

where X is caused by the presence of interferer in the communication medium, which includes both the received signal power generated by the interferer nodes and the noise power caused by the interferer signal.

Another important observation is that the distances from any interferer to the targeted receiver are Independent and Identically Distributed (IID). For a sufficiently large number of users, the Central Limit Theorem can be invoked and the Gaussian assumption can be made for X, when estimating the aggregate interference [9]. Therefore, the moments of the interference from a single node are first determined and then the Central Limit Theorem is applied to approximate the aggregated interference.

With respect to the dense nano-networks with the adoption of TS-OOK as the communication scheme, a collision between symbols will occur when they reach the receiver at the same time and overlap. The probability of having an arrival during T_s seconds is a uniform random probability distribution with pdf equal to $1/T_s$ [9]. Therefore, for a specific transmission, a collision will happen with a probability $2T_p/T_s$ (with an assumption that a correlation-based energy detector is used at the receiver) [9].

It is noted that not all types of symbols harmfully collide, only pulses (logical "1"s) create interference because the molecular absorption noise is signal power-dependent. It is assumed that all nano-nodes in the transmission area share the same pulse transmitting probability. Therefore, the node density parameter λ in (5) can be replaced by [10],

$$\lambda' = \lambda_T(2T_p/T_s)p_1 \quad (12)$$

where λ_T refers to the density of active nodes in $nodes/m^2$, T_p is the symbol duration, T_s is the time between symbols, and p_1 denotes the probability of a nano-machine to transmit a pulse. This expression highlights the fact that transmission of logical "0" does not generate interference to other ongoing transmissions. Both the interference caused by the interfering nodes in the transmission area and the interference generated by the utilisation of TS-OOK are taken into account in (12).

This article has been accepted for publication in a future issue of this journal, but has not been fully edited. Content may change prior to final publication. Citation information: DOI 10.1109/ACCESS.2017.2713459, IEEE Access

1) Single Node Interference Model: For a Poisson Point Process, any given number of interferer in a disc of radius R are independently and uniformly distributed. Therefore, the distance to the targeted receiver, denoted as a random variable D, has the same pdf for any interferer node,

$$f_D(r) = 2r/R^2, 0 < r < R \tag{13}$$

Now consider a random variable $G = 1/D^2$. Under Poisson assumption, the moments of G can be written as [27],

$$E[G^\theta] = \int_0^R \frac{2x}{R^2}(\frac{1}{x^2})^\theta dx \tag{14}$$

The integral does not converge because it is unbounded approaching zero from the right. To deal with this issue, it is assumed that the transmitters cannot be located closer than a certain very small distance a from the receiver. This assumption is warranted from the practical point of view, especially, taking into account that a can be chosen as small as required [11]. Thus, the distribution of the distance to the targeted receiver could be approximated as the distance from a point arbitrarily distributed in the region bounded by two concentric circles of radius a and R, $R > a$, to their common centre. It is known to be [12],

$$f_D(r) = 2r/(R^2 - a^2), a < r < R \tag{15}$$

The first moment of variable G is computed as,

$$E[G] = \int_a^R \frac{2x}{(R^2 - a^2)}\frac{1}{x^2}dx = \frac{2(lnR - lna)}{R^2 - a^2} \tag{16}$$

Similarly, the variance of G is calculated to be,

$$\sigma^2[G] = \frac{1}{a^2R^2} - 4(\frac{lnR - lna}{R^2 - a^2})^2 \tag{17}$$

The interference model for a single node has been obtained, and then it is moved to the aggregate interference. The stochastic sum of random variables G is considered in (11).

2) Aggregate Interference Model: It is assumed that the number of interferer is exactly k, which results in conditional moment of X to be [12],

$$E[X(\vec{r})|M = k] = A\sum_{i=1}^{k} E[G_i] = AkE[G] \tag{18}$$

Denoting $P_r(M = k) = p_k$ and unconditioning (18) gives,

$$E[X(\vec{r})] = A\sum_{k=0}^{\infty} p_k kE[G] = AE[G]E[M] \tag{19}$$

Similarly, the second conditional moment of X is given by,

$$\begin{aligned} E[X^2(\vec{r})|M = k] &= A^2E[(\sum_{i=1}^{k} r_i^{-2})^2] \\ &= A^2\sum_{i=1}^{k}\sum_{j=1}^{k}(E[G_i]E[G_j] + K_{ij}) \end{aligned} \tag{20}$$

where $K_{ij} = Cov(G_i, G_j)$ is the pairwise covariance. Since G_i and G_j are pairwise independent $K_{ij} = 0, i = 1, , 2, \ldots, k, i \neq j$ and $K_{ii} = \sigma^2[G_i], i = 1, 2, ..., k$ [10]. Further, since all G_i identically distributed,

$$E[G_i] = E[G_j], \sigma^2[G_i] = \sigma^2[G_j] \tag{21}$$

Thus, after unconditioning (20),

$$E[X^2(\vec{r})] = A^2((E[G])^2E[M^2] + \sigma^2[G]E[M]) \tag{22}$$

Then the variance of X can be found as,

$$\sigma^2[X(\vec{r})] = A^2((E[G])^2\sigma^2[M] + \sigma^2[G]E[M]) \tag{23}$$

In (10) the moments of random variable X are being calculated; thus, pdf of SINR in dB can be obtained based on conventional methods of finding distributions of functions of random variables. Recall that pdf of a random Y, $w(f)$, expressed as monotonous function $y = \phi(x)$ of another random variable $X$with pdf $f(x)$ is given by [28],

$$w(y) = f(\psi(y))|\psi'(y)| \tag{24}$$

where $x = \psi(y) = \phi^{-1}(x)$is the inverse function.

The inverse of $y = \phi(x) = 10log_{10}(P_R/(N_m + x))$ is unique and monotonous and given by $x = \psi(y) = P_R10^{-y/10} - N_m$. The modulo of the derivative is $|\psi'(y)| = |P_R10^{-y/10}ln(10^{-1/10})|$. Substituting these into (27), pdf of logarithm of SINR is,

$$w_{logS}(y) = \frac{|P_R10^{-y/10}ln(10^{-1/10})|}{\sqrt{2\pi}\sigma}e^{-\frac{(P_R10^{-y/10} - N_m - \mu)^2}{2\sigma^2}} \tag{25}$$

where $\mu = E[X(\vec{r})], \sigma^2 = \sigma^2[X(\vec{r})]$ can be obtained in (19) and (23)

V. Analytical Results

Based on the aforementioned derived models, it is noted that the distribution and average values of SINR are directly dependent of the node density and probability of transmitting pulses. In this section, we analytically investigate the effect of these parameters on the system performance of in-vivo nano-networks inside three human tissues (blood, skin and fat).

The simulation environment of following analytical study is summarised in Table. 1.

Table I
Simulation environment

Parameters	Definition
$R = 3mm$	The radius of the considered disc.
$r_0 = 1mm$	The distance between the targeted transmitter and the targeted receiver.
$T_0 = 310K$	The temperature of human tissues, and tissues are assumed as isothermal.
$P_T = 1pJ$	The total energy of the transmitted Gaussian pulse.
$B = 1THz$	The bandwidth of the transmitted Gaussian pulse.
$T_p = 100fs$	The pulse duration of the transmitted Gaussian pulse.
$n = 6$	The derivative order of the transmitted Gaussian pulse.
$\sigma = 0.15$	The standard deviation of the transmitted Gaussian pulse.

With respect to TS-OOK, it is envisioned $T_s/T_p = 100$ in (12) to satisfy the requirement with regards to the time

This article has been accepted for publication in a future issue of this journal, but has not been fully edited. Content may change prior to final publication. Citation information: DOI 10.1109/ACCESS.2017.2713459, IEEE Access

between symbols, which should be much longer than the symbol duration. Aforementioned, the node density of WNSNs can be hundreds of nano-sensors per millimetre. Therefore, $\lambda_T = 10, 100$, and 1000 $nodes/mm^2$ are chosen to evaluate the effect of the interfere density on the system performance.

A. SINR Distribution

Fig. 4 shows the result for SINR distribution at different node densities with a specific signal transmission probability $p_1 = 0.5$ for THz wave communicating inside human blood, skin and fat tissues.

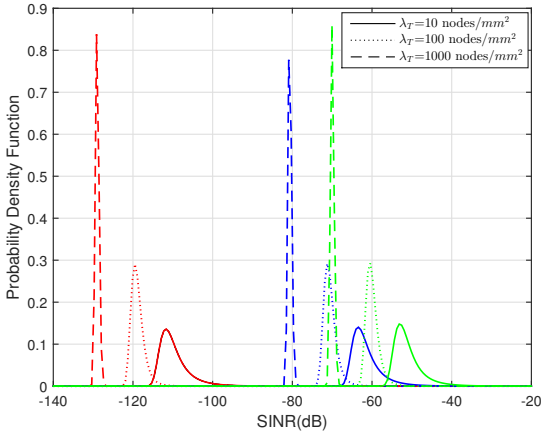

Figure 4. Probability density function of SINR for different node densities λ_T when p_1=0.5 in human blood (red), skin (blue) and fat (green)

As expected, it can be concluded that for a specific probability of transmitting pulses, SINR decreases significantly with the increase of node density. Specifically, SINR created by a Poisson field of nano-devices with parameter $\lambda_T = 10$ $nodes/mm^2$ which are operating under the previous conditions in human blood, has an average power of approximately -115 dB. When the node density is increased to $\lambda_T = 100$ $nodes/mm^2$ and $\lambda_T = 1000$ $nodes/mm^2$, the values reduce to -120 dB and -130 dB, respectively. The reason is that collisions occur with a higher probability, when interferer nodes grow in the communication area. Similarly, THz communication in human skin and fat experiences this trend because more interference could be caused with the presence of larger number of nodes. Specifically, in the human skin scenario, the SINR values decrease from about -63 dB to -70 dB and to -80 dB with node densities increasing. And for human fat, the values are about -52 dB, -61 dB and -70 dB when node densities are $\lambda_T = 10 nodes/mm^2$, $\lambda_T = 100 nodes/mm^2$ and $\lambda_T = 1000 nodes/mm^2$, respectively. Differently, the SINR in human blood is the worst case among these mediums, because blood has the highest water concentration and the molecular absorption is dominantly contributed by the molecules of water vapour [4].

Fig. 5 illustrates the effect of probability of transmitting pulses on the distribution of SINR for the communication system. For a specific node density $\lambda_T = 100$ $nodes/mm^2$, by increasing the probability p_1 from 0.1 to 0.9, the average SINR of nano-networks in human blood decreases from -112 dB to -119 dB to -122 dB. Similarly, for communication inside human skin, the average SINR value goes down from -65 dB to -71 dB and then to -73 dB when the probability grows. In fat scenario, a descending trend happens from -56 dB to -61 dB and then to -63 dB with the increase of the probability. These results emphasise the fact that the molecular absorption noise and multi-user interference are directly dependent of the transmitted signal, thus the transmitting pulses potentially degrade the communication system performance. These results depict that the degradation effect which is caused by both the molecular absorption noise and interference can be mitigated by using lower transmission probability and prevent transmission errors from occurring at the beginning.

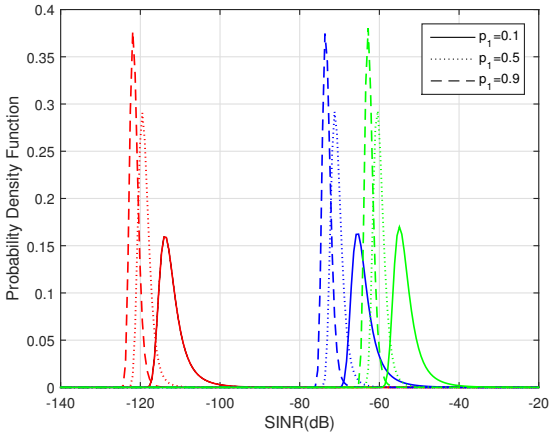

Figure 5. Probability density function of SINR for different probability of transmitting pulses p_1 when $\lambda_T = 100$ $nodes/mm^2$ in human human blood (red), skin (blue) and fat (green)

B. Mean SINR Assessment

In this section, the effect of the node densities and probabilities of transmitting pulses on in-vivo nano-communication at the THz band is studied. The communication happens between a deterministic targeted transmitter and receiver with random interfering nodes in the communication area inside all three human tissues (blood, skin and fat). The communication performance especially the achievable communication range is evaluated, by investigating the dependence of the mean values of SINR on the transmission distance in different human tissues.

1) Effect of Node Density: The mean SINR for scenarios with three different node densities in the communication area is illustrated in Fig. 6. It can be clearly seen that SINR steadily decreases with the transmission distance and the rise of node density for THz communication in all three kinds of communication medium. More specifically, SINR degrades about 10 dB, when the node density increases one order.

2) Effect of Pulses Probability: The effect of the probability of transmitting pulses on the mean SINR of THz communication inside human tissues is shown in Fig. 7. It is presented that average SINR degrades with the communication distance and the pulses probability regardless of the medium type.

This article has been accepted for publication in a future issue of this journal, but has not been fully edited. Content may change prior to final publication. Citation information: DOI 10.1109/ACCESS.2017.2713459, IEEE Access

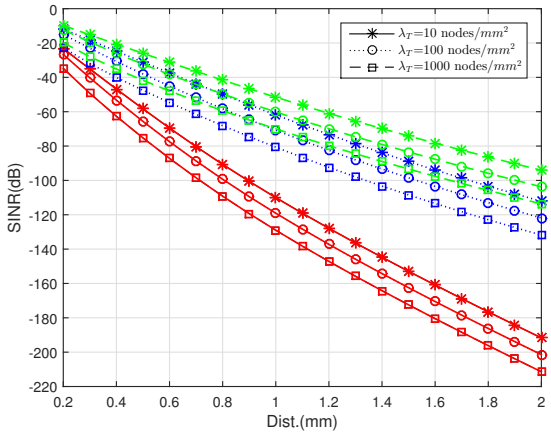

Figure 6. Average SINR versus communication distance for different node densities in the communication area in human blood (red), skin (blue) and fat (green) tissues

Specifically, the SINR drops approximate 5 dB, when the pulses transmission probability rises from 0.1 to 0.5, and SINR degrades about 2 dB, when the pulses transmission probability increases from 0.5 to 0.9, respectively.

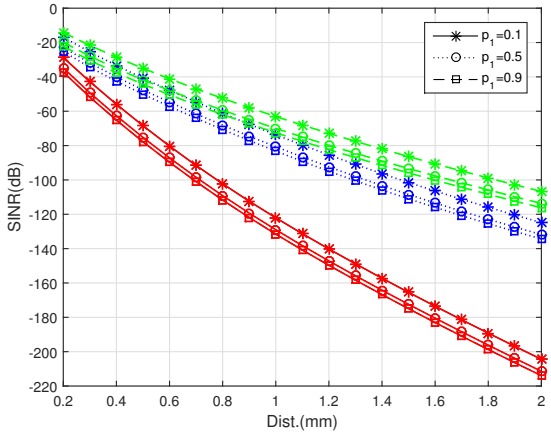

Figure 7. Average SINR versus communication distance for different probabilities of transmitting pulses of THz communication in human blood (red), skin (blue) and fat (green) tissues

One significant observation from both Fig. 6 and Fig. 7 is that the maximum achievable transmission distance to enable simultaneous communications is strictly constrained. In light of the state of the art in nano-communication devices and to an extent to make the in-vivo THz nano-networks realistic, such low SINR limits the communication range to about 1 mm, and more specific distance depends on the communication medium composition, node density in the area and probability of transmitting pulses. Considering the scale of the nano-devices, this transmission distance is enough to enable the envisioned nano-communication for power and complexity constrained body-centric nano-network at the THz band.

More importantly, The obtained results imply that by controlling the pulse transmitting probability and node density, the interference can be reduced and SINR of the in-vivo nano-communication system can be bettered. Practically, a trade-off can be made between node density and pulse transmitting probability to achieve the expected communication performance.

VI. Conclusion

In this paper, the feasibility of TS-OOK communication scheme for in-vivo nano-networks at the THz band is first demonstrated. Subsequently, a preliminary network-level analytical model for this in-vivo nano-networks with the utilisation of TS-OOK is proposed based on the mathematical apparatus of stochastic geometry. Without loss of generality, the developed model is valid to any power allocation schemes. The performance of multi-user communication inside human blood, skin and fat is comparatively illustrated, showing that blood is the worst performing scenario because of high water concentration in human blood than skin and fat. In all three kinds of tissues, the obtained results indicates that high node density and pulse transmission probability would potentially decrease SINR of the system and impair the system performance. The effective communication distance for dense nano-networks inside the human body is restrained to about 1 mm, and more specific achievable range depends on the particular transmission environment. Moreover, it is analytically shown that the system performance can be improved by controlling the node density of nano-machines in the communication field and the pulse transmission probability. In particular, SINR improves about 10 dB, when the node density decreases one order and SINR improves approximate 5 dB and 2 dB, when the probability drops from 0.5 to 0.1 and 0.9 to 0.5, respectively. The presented results provide important basis for more practically network-level modelling with consideration of antenna directivity and None Line of Sight (NLoS) paths. This study also stimulates further research on simple, reliable and energy efficient communication protocols and coding schemes, and provide an important contribution to the achievement of THz in-vivo nano-networks.

VII. Acknowledgement

Many thanks to the CSC (China Scholarship Council) (No. 201506290051) for supporting the first author's research studies at Queen Mary University of London (QMUL), UK. This publication was made possible by NPRP grant # 7-125-2-061 from the Qatar National Research Fund (a member of Qatar Foundation). The statements made herein are solely the responsibility of the authors.

References

[1] I. F. Akyildiz and J. M. Jornet, "Electromagnetic wireless nanosensor networks," *Nano Communication Networks*, vol. 1, no. 1, pp. 3–19, 2010.

[2] I. F. Akyildiz and J. M. Jornet, "The internet of nano-things," *IEEE Wireless Communications*, vol. 17, no. 6, pp. 58–63, 2010.

[3] Q. Abbasi, K. Yang, N. Chopra, J. Jornet, N. A. AbuAli, K. Qaraqe, and A. Alomainy, "Nano-communication for biomedical applications: A review on the state-of-the-art from physical layers to novel networking concepts," *IEEE Access Journal*, vol. 4, pp. 3920–3935, 2016.

[4] J. M. Jornet and I. F. Akyildiz, "Channel modeling and capacity analysis for electromagnetic wireless nanonetworks in the terahertz band," *Wireless Communications, IEEE Transactions on*, vol. 10, no. 10, pp. 3211–3221, 2011.

[5] K. Yang, A. Pellegrini, A. Brizzi, A. Alomainy, and Y. Hao, "Numerical analysis of the communication channel path loss at the thz band inside the fat tissue," in *Microwave Workshop Series on RF and Wireless Technologies for Biomedical and Healthcare Applications (IMWS-BIO), 2013 IEEE MTT-S International*, pp. 1–3, 2013.

[6] P. Boronin, D. Moltchanov, and Y. Koucheryavy, "A molecular noise model for thz channels," in *Communications (ICC), 2015 IEEE International Conference on*, pp. 1286–1291, 2015.

[7] Q. H. Abbasi, H. El Sallabi, N. Chopra, K. Yang, K. A. Qaraqe, and A. Alomainy, "Terahertz channel characterization inside the human skin for nano-scale body-centric networks," *IEEE Transactions on Terahertz Science and Technology*, vol. 6, no. 3, pp. 427–434, 2016.

[8] J. M. Jornet and I. F. Akyildiz, "Femtosecond-long pulse-based modulation for terahertz band communication in nanonetworks," *Communications, IEEE Transactions on*, vol. 62, no. 5, pp. 1742–1754, 2014.

[9] J. M. Jornet and I. F. Akyildiz, "Low-weight channel coding for interference mitigation in electromagnetic nanonetworks in the terahertz band," in *2011 IEEE International Conference on Communications (ICC)*, pp. 1–6, 2011.

[10] J. M. Jornet, "Low-weight error-prevention codes for electromagnetic nanonetworks in the terahertz band," *Nano Communication Networks*, vol. 5, no. 1, pp. 35–44, 2014.

[11] V. Petrov, D. Moltchanov, and Y. Koucheryavy, "On the efficiency of spatial channel reuse in ultra-dense thz networks," in *2015 IEEE Global Communications Conference (GLOBECOM)*, pp. 1–7, 2015.

[12] V. Petrov, D. Moltchanov, and Y. Koucheryavy, "Interference and sinr in dense terahertz networks," in *Vehicular Technology Conference (VTC Fall), 2015 IEEE 82nd*, pp. 1–5, 2015.

[13] V. Petrov, M. Komarov, D. Moltchanov, J. M. Jornet, and Y. Koucheryavy, "Interference and sinr in millimeter wave and terahertz communication systems with blocking and directional antennas," *IEEE Transactions on Wireless Communications*, vol. 16, no. 3, pp. 1791–1808, 2017.

[14] J. M. Jornet and I. F. Akyildiz, "Channel capacity of electromagnetic nanonetworks in the terahertz band," in *Communications (ICC), 2010 IEEE International Conference on*, pp. 1–6, 2010.

[15] P. Boronin, V. Petrov, D. Moltchanov, Y. Koucheryavy, and J. M. Jornet, "Capacity and throughput analysis of nanoscale machine communication through transparency windows in the terahertz band," *Nano Communication Networks*, vol. 5, no. 3, pp. 72–82, 2014.

[16] K. Yang, A. Pellegrini, M. O. Munoz, A. Brizzi, A. Alomainy, and Y. Hao, "Numerical analysis and characterization of thz propagation channel for body-centric nano-communications," *IEEE Transactions on Terahertz Science and technology*, vol. 5, no. 3, pp. 419–426, 2015.

[17] Q. H. Abbasi, A. Alomainy, M. U. Rehman, and K. Qaraqe, *Advances in Body-Centric Wireless Communication: Applications and State-of-the-Art*. The Institution of Engineering and Technolog (IET) Publication, 2016.

[18] A. Fitzgerald, E. Berry, N. Zinov'ev, S. Homer-Vanniasinkam, R. Miles, J. Chamberlain, and M. Smith, "Catalogue of human tissue optical properties at terahertz frequencies," *Journal of Biological Physics*, vol. 29, no. 2-3, pp. 123–128, 2003.

[19] E. Berry, A. J. Fitzgerald, N. N. Zinov'ev, G. C. Walker, S. Homer-Vanniasinkam, C. D. Sudworth, R. E. Miles, J. M. Chamberlain, and M. A. Smith, "Optical properties of tissue measured using terahertz-pulsed imaging," in *Medical Imaging 2003*, pp. 459–470, International Society for Optics and Photonics, 2003.

[20] R. Zhang, K. Yang, A. Alomainy, Q. H. Abbasi, K. Qaraqe, and R. M. Shubair, "Modelling of the terahertz communication channel for in-vivo nano-networks in the presence of noise," in *Microwave Symposium (MMS), 2016 16th Mediterranean*, pp. 1–4, IEEE, 2016.

[21] R. Zhang, K. Yang, Q. H. Abbasi, K. A. Qaraqe, and A. Alomainy, "Analytical modelling of the effect of noise on the terahertz in-vivo communication channel for body-centric nano-networks," *Nano Communication Networks*, 2017.

[22] E. Zarepour, M. Hassan, C. T. Chou, and S. Bayat, "Performance analysis of carrier-less modulation schemes for wireless nanosensor networks," in *Nanotechnology (IEEE-NANO), 2015 IEEE 15th International Conference on*, pp. 45–50, 2015.

[23] J. M. Jornet and I. F. Akyildiz, "Graphene-based plasmonic nano-transceiver for terahertz band communication," in *The 8th European Conference on Antennas and Propagation (EuCAP 2014)*, pp. 492–496, 2014.

[24] H. ElSawy, E. Hossain, and M. Haenggi, "Stochastic geometry for modeling, analysis, and design of multi-tier and cognitive cellular wireless networks: A survey," *IEEE Communications Surveys & Tutorials*, vol. 15, no. 3, pp. 996–1019, 2013.

[25] J. G. Andrews, R. K. Ganti, M. Haenggi, N. Jindal, and S. Weber, "A primer on spatial modeling and analysis in wireless networks," *IEEE Communications Magazine*, vol. 48, no. 11, pp. 156–163, 2010.

[26] D. R. Cox and V. Isham, *Point processes*, vol. 12. CRC Press, 1980.

[27] A. Papoulis and S. U. Pillai, *Probability, random variables, and stochastic processes*. Tata McGraw-Hill Education, 2002.

[28] W. Feller, *An introduction to probability theory and its applications: volume I*, vol. 3. John Wiley & Sons London-New York-Sydney-Toronto, 1968.